

# $[\text{PdCl}_2(\text{NH}_2(\text{CH}_2)_{12}\text{CH}_3)_2]$ supported on an active carbon: effect of the carbon properties on the catalytic activity of cyclohexene hydrogenation

J.A. Díaz-Auñón<sup>a</sup>, M.C. Román-Martínez<sup>a</sup>, C. Salinas-Martínez de Lecea<sup>a,\*</sup>,  
P.C. L'Argentièrè<sup>b</sup>, E.A. Cagnola<sup>b</sup>, D.A. Liprandi<sup>b</sup>, M.E. Quiroga<sup>b</sup>

<sup>a</sup> *Departamento de Química Inorgánica, Facultad de Ciencias, Universidad de Alicante, Apdo. de Correos 99, Alicante 03080, Spain*

<sup>b</sup> *Química Inorgánica – INCAPE, Facultad de Ingeniería Química, Universidad Nacional del Litoral – CONICET, Santiago del Estero 2829, 3000 Santa Fe, Argentina*

Received 13 July 1999; accepted 13 September 1999

## Abstract

The catalytic activity and poisoning resistance of  $[\text{PdCl}_2(\text{NH}_2(\text{CH}_2)_{12}\text{CH}_3)_2]$ , supported on active carbons, have been studied, regarding the effect of some of the support properties, such as: porosity, surface chemistry and sulphur content. Commercial active carbons and almond-shell-derived carbons were used. Some of the commercial active carbons were submitted to different treatments to purify them or to modify the support surface chemistry. Active carbons were characterised by nitrogen adsorption at 77 K, carbon dioxide adsorption at 273 K, mercury porosimetry, elemental analysis and TPD. Catalysts were prepared supporting the metal complex by the incipient impregnation method, with a palladium content of ca. 0.3% wt. All the catalysts were analysed by XPS and nitrogen adsorption at 77 K. The catalytic activity and sulphur-poisoning resistance were determined in the cyclohexene hydrogenation to cyclohexane. Tetrahydrothiophene (THT) was used as the poisoning agent in a concentration of 300 ppm. Regarding the effect of support porosity, the catalytic activity increases with supermicropore ( $\varnothing$  from 0.7 to 2 nm) volume. With regard to the oxygen surface groups and sulphur content of the active carbons, no effect has been found. Catalyst poisoning by THT is found to be independent of the active carbon properties and lower than that observed for the unsupported metal complex and the complex supported on  $\gamma\text{-Al}_2\text{O}_3$ . © 2000 Elsevier Science B.V. All rights reserved.

**Keywords:** Carbon; Cyclohexene hydrogenation;  $[\text{PdCl}_2(\text{NH}_2(\text{CH}_2)_{12}\text{CH}_3)_2]$

## 1. Introduction

Transition metal complexes have been extensively used as catalysts for hydrogenation reactions, not only in the homogeneous but also in the heterogeneous phase [1–3].

The advantage of supported metal complexes over unsupported ones is the ease of separating them from the reaction media, which makes them economically more convenient. These supported metal complexes show also the advantage of a good performance in mild conditions [4].

Palladium metal complexes have been widely used in hydrogenation reactions, mostly in ho-

\* Corresponding author.

mogeneous selective hydrogenation reactions of conjugated dienes [5–9]. However, despite their scientific and industrial importance, only a few papers have been written on palladium complexes in heterogeneous reactions [10–15].

In previous papers, the catalytic activity of the  $[\text{PdCl}_2(\text{NH}_2(\text{CH}_2)_{12}\text{CH}_3)_2]$  complex was studied for the cyclohexene to cyclohexane hydrogenation in homogeneous and heterogeneous phase using alumina and carbon as supports, with and without the addition of the poisoning agent tetrahydrothiophene (THT) [13–15]. The catalyst resistance to poisoning by sulphur compounds is an important property because their presence is quite common in the hydrocarbon distillates. THT is an example of a strong poisoning agent for different catalysts. Besides, in the case of the  $[\text{PdCl}_2(\text{NH}_2(\text{CH}_2)_{12}\text{CH}_3)_2]$  complex, the THT presents a poisoning mechanism different from that shown by other sulphur compounds [1,6]. In this case, there is an amine ligand substitution instead of a competitive adsorption with  $\text{H}_2$  or the substrate (such as in the thiophene case). All these means an alteration of the electronic structure of the metal complex with the consequence of its irreversible destruction. On the other hand, a possible lixiviation of the  $[\text{PdCl}_2(\text{NH}_2(\text{CH}_2)_{12}\text{CH}_3)_2]$  complex was taken into account [14], but no washing of the metal complex by the solvent used was observed during the process. Results also showed that catalysts supported on carbon have higher catalytic activity and THT resistance; even more, some of the samples have a catalytic activity in the presence of THT, which is almost twice the value obtained for unsupported  $[\text{PdCl}_2(\text{NH}_2(\text{CH}_2)_{12}\text{CH}_3)_2]$ .

In the papers mentioned [14,15], it was not possible to determine which carbon properties are responsible of such interesting results. Because of this, the purpose of this paper is to carry out a deeper and exhaustive study on the effect of the carbon properties related to the catalytic activity. To pursue this goal, several carbon materials with different characteristics (porosity, specific surface area, sulphur content

and surface chemistry) were used with the objective of analysing the effect of each variable independently.

## 2. Experimental

### 2.1. Preparation of supports

Two active carbons were obtained from almond shells by carbonization at 1123 K (char B) and an ulterior physical activation with  $\text{CO}_2$  (called BC-32 and BCaC-30) [16]. In this way, two active carbons were got free of S and very suitable to be used as catalysts supports. Another three pelletized commercial carbons (ROX-0.8, RX-3 and GF-45, from NORIT), with different particle size and textural properties were used. From ROX-0.8, three extra carbon samples were prepared. Sample ROX-N was obtained by oxidation of ROX-0.8 with  $\text{HNO}_3$  35% [17], sample ROX-NT was obtained by a heat treatment at 773 K of ROX-N in an inert atmosphere [18], and ROX-SF was obtained by successive treatment of ROX-0.8 with HCl,  $\text{HNO}_3$ , and HF (all of them at a concentration of 10%) to remove mineral matter and subsequent heating at 1123 K in hydrogen during 12 h to eliminate organic sulphur [19].

### 2.2. Characterization of supports

Physical adsorption of gases ( $\text{N}_2$  at 77 K and  $\text{CO}_2$  at 273 K) and mercury porosimetry were used to analyze the porous texture of carbons.

Gas physical adsorption is useful to calculate specific surface area and pore volume. The use of both adsorptives ( $\text{N}_2$  and  $\text{CO}_2$ ) allows to estimate the pore volume distribution of pores up to about 7.5 nm diameter [20]. By applying the Dubinin–Raduskevich equation [21] to the  $\text{CO}_2$  adsorption isotherm at 273 K, the volume of micropores with a diameter less than 0.7 nm ( $V_{\text{micro}}$ ) can be obtained. On the other hand, the volume of supermicropores ( $V_{\text{sm}}$ ), diameter ranging from 0.7 to 2 nm, is obtained by subtraction of  $V_{\text{micro}}$  to the volume calculated by

applying the Dubinin–Raduskevich method to the  $N_2$  adsorption isotherm at 77 K [20]. The wider the porosity, macropores ( $V_{\text{macro}}$ ) and part of the mesopores (with diameter from 7.5 to 50 nm), was determined by mercury porosimetry, using a Carlo Erba 2000 porosimeter. This equipment reaches a maximum pressure of 2000 kg/cm<sup>2</sup>, what allows to estimate the volume of pores with a diameter longer than 7.5 nm. The volume of mesopores with diameter between 2 and 7.5 nm was calculated from the  $N_2$  adsorption isotherm at 77 K. To this respect, the volume of gas adsorbed between 0.2 and 0.7 relative pressure corresponds to the mesopore range of porosity. The addition of the mesopore volume determined from  $N_2$  adsorption isotherm and determined by Hg porosimetry gives the total mesopore volume ( $V_{\text{meso}}$ ) [20]. Finally, with the B.E.T. equation [22] applied to the  $N_2$  adsorption isotherm at 77 K is possible to evaluate the specific surface area.

TPD experiments were used to study surface chemistry by analyzing the evolution of desorbed gases (CO and CO<sub>2</sub>), during a thermal treatment in an inert atmosphere, with a VG Quadrupole Mass Spectrometer. The experiments were carried out heating the samples in a He flow at 20 K/min up to 1173 K. Both CO and CO<sub>2</sub> are originated from the oxygen groups decomposition, which are present on the carbon surface [18,23]. The CO observed by TPD comes from slightly acidic or neutral groups (phenols, carbonyls and quinones), while CO<sub>2</sub> is the decomposition product of acidic groups like carboxylic, lactone or anhydride [18,24]. The surface chemistry of the carbon material is also reflected by the acid–base character. In our case, an approximation to the acid–base properties of the selected supports was obtained by measuring the pH of their aqueous suspension (1 g of carbon/10 ml of distilled water) [25].

Elemental analysis in an EAGER-2000 equipment was also used to assess organic sulphur, while ashes (% Cz) were determined by burning off the carbon material at 1023 K and weighting the residue.

### 2.3. Metal complex synthesis and preparation of catalysts

As previously reported [13], the  $[PdCl_2-(NH_2(CH_2)_{12}CH_3)_2]$  complex was prepared by reaction of  $PdCl_2$  with  $CH_3(CH_2)_{12}NH_2$  in toluene, in a glass equipment with stirring and reflux, under a purified argon atmosphere at 338 K, during 4 h and with a molar ratio  $CH_3(CH_2)_{12}NH_2:Pd = 2$ . The solid phase disappeared after 1 h ( $PdCl_2$  is insoluble in toluene) and, simultaneously, a yellow-orange colour appeared in the liquid phase. Upon ending the reaction, the solvent was evaporated and a yellow solid was obtained, which was very different from the brown coloured  $PdCl_2$ . In parallel, and as a test experiment, the same procedure was followed using only  $PdCl_2$  in toluene. In this case, no colour changes were observed and the initial separation of phases was maintained. This proves that  $CH_3(CH_2)_{12}NH_2$  had effectively reacted with  $PdCl_2$  to give the metal complex species.

The final purification of the metal complex was made by column chromatography, using silica-gel as stationary phase and chloroform as solvent. All the aliquots obtained were analyzed by thin layer chromatography using silica-gel as support, chloroform–methanol (in a molar ratio 6:1) as a mobile phase and potassium dichromate in concentrated sulphuric acid as a revealing reagent.

Heterogeneization of the palladium complex (named TDA in the following considerations) was carried out by means of the incipient wetness technique [26]. A solution of the palladium complex in toluene in a suitable concentration to obtain a catalyst containing 0.3% Pd was used for impregnation.

### 2.4. Characterization of complex and catalysts

Catalytic activity and sulphur resistance were determined in a stirred tank reactor operated at 353 K and stirring velocity of 600 rpm. No diffusion limitations were observed under these

conditions [27]. The hydrogenation of cyclohexene to cyclohexane was used as a test reaction. A hydrogen pressure of 500 kPa and a solution of 5% cyclohexene in toluene (hereafter PF, poison-free) were the reactants used. To study the poisoning effect, 300 ppm of THT were added to the PF solution. In all cases, 0.2 g of catalysts were used. In the homogeneous experiments, a similar quantity of the metal complex present in the heterogeneous tests was dissolved in the cyclohexene–toluene solution. The molar rate THT/Pd was 2/1 approximately. The hydrogenation reaction was carried out for 3 h. Reactants and products were chromatographically analyzed using a Konic 3000 equipment with a FID detector and a CP Sill 88 capillary column. The catalytic activity was expressed as the kinetic constant,  $k$ , determined as the slope of the conversion vs. time plot, assuming a zero order reaction respect to  $P_{H_2}$  [28]. The relative experimental error was about 3%. The relative decrease in activity values after poisoning ( $R_{THT}$ ), was determined from the activity data obtained with the PF solution ( $k_{PF}$ ) and with the

solution containing THT ( $k_{THT}$ ), calculated as:  $R_{THT} = (k_{PF} - k_{THT}) / (k_{PF}) * 100$ . In all cases, the selectivity to cyclohexane was 100%.

The THT adsorption on carbon was studied by putting in contact 0.2 g of active carbon with 100 ml of a solution containing 300 ppm of THT in toluene, at 353 K for 3 h. Afterwards, the concentration of THT in the solution was analyzed by MS-GC.

The electronic state of Pd, N and Cl and their atomic ratios in the supported and unsupported metal complex, as well as the state of C in the carbon supports and the presence of S in the poisoned samples were studied by X-ray Photoelectron Spectroscopy (XPS). Determinations were carried out on a Shimadzu ESCA 750 electron spectrometer coupled to a Shimadzu ESCAPAC 760 Data System. In order to correct possible deviations caused by electric charge of the samples, the C 1s line was taken as an internal standard at 285.0 eV, as previously described [26]. The samples were introduced into the XPS equipment sample holder following the operational procedure described by other

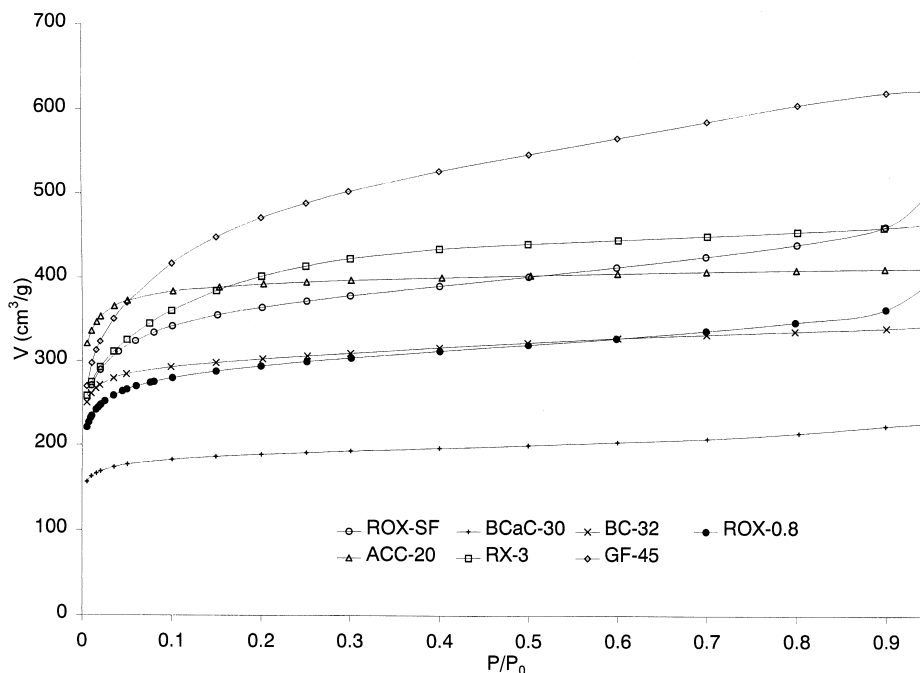


Fig. 1.  $N_2$  adsorption isotherms at 77 K of carbon supports.

authors [29] in order to ensure that there was no modification on the electronic states of the species analysed [30]. Anyhow, exposing the samples to the atmosphere for different periods confirmed that there were no electronic modifications. Determinations of the surface atomic ratios  $X/Pd$  ( $X = N, Cl$  and  $S$ ) were made by comparing the areas under the peaks after background subtraction and corrections due to differences in escape depths and in photoionization cross-sections [31].

### 3. Results

#### 3.1. Characterization of supports

Fig. 1 shows the  $N_2$  adsorption isotherms at 77 K obtained for all the carbons used as supports. They present a variety of shapes, although all of them show a high contribution of micropores. The isotherms corresponding to GF-45, ROX-SF and ROX-0.8 samples have a strong slope between 0.2 and 0.7 of relative pressure ( $P/P_0$ ), what indicates an important contribution of mesopores [20]. The shape of the isotherm of the sample RX-3 reveals the presence of abundant narrow mesopores and supermicropores, while there is a scarce presence of larger pores. BC-32 and BCaC-30 carbons have mainly micropores although mesopores are also present to some extent. The isotherms corresponding to ROX-N and ROX-NT carbons, not

Table 2  
Characterization of the supports used

Support	% S	% Cz	pH	CO ( $\mu\text{mol/g}$ )	CO <sub>2</sub> ( $\mu\text{mol/g}$ )
ROX-0.8	0.43	2.81	7.23	88	168
ROX-N	0.29	2.32	3.68	1485	638
ROX-NT	0.27	2.28	7.89	576	107
RX-3	0.31	1.59	7.13	153	67
GF-45	0.00	5.50	5.86	461	438
BC-32	0.00	0.15	8.30	157	76
BCaC-30	0.00	0.06	7.53	394	60
ROX-SF	0.00	–	–	588	605

shown in Fig. 1, are coincident with that found for ROX-0.8.

Table 1 shows the estimated specific surface area and pore volume data. As can be observed, the selected samples show a wide range of specific surface area (between 580 and 1700  $\text{m}^2/\text{g}$ ) and pore size distribution.

Table 2 shows sulphur (% S) and ash (% Cz) contents, aqueous suspension pH, and CO and CO<sub>2</sub> evolution in TPD experiments for the different carbons. From this table, it can be seen that some carbons contain some sulphur (RX-3, ROX-0.8, ROX-N and ROX-NT), what could have a negative influence on the catalytic activity. On the other hand, all the other active carbons possess a sulphur content undetectable by the experimental technique used. Ash content results show that the GF-45 sample has the highest percentage of Cz value, while the active carbons prepared from almond shell char (BC-32 and BCaC-30) present the lowest ash content. The pH and TPD data indicate that in what

Table 1  
Specific surface area and porosity distribution

Support	$S_{\text{BET}}$ ( $\text{m}^2/\text{g}$ )	$V_{\text{micro}}$ ( $\text{cm}^3/\text{g}$ )	$V_{\text{sm}}$ ( $\text{cm}^3/\text{g}$ )	$V_{\text{meso}}$ ( $\text{cm}^3/\text{g}$ )	$V_{\text{macro}}$ ( $\text{cm}^3/\text{g}$ )
ROX-0.8	934	0.365	0.093	0.152	0.410
ROX-N	958	0.399	0.065	–	–
ROX-NT	935	0.376	0.091	–	–
ROX-SF	1179	0.416	0.168	0.236	0.490
BC-32	935	0.381	0.088	0.112	0.160
RX-3	1411	0.356	0.333	0.098	0.430
BCaC-30	584	0.279	0.010	0.093	0.090
GF-45	1718	0.345	0.498	0.449	0.400

concerns to surface chemistry, the selected carbons can be divided in two groups: ROX-N, GF-45 and ROX-SF with an acidic behaviour and a high content of surface oxygen complexes, and RX-3, ROX-0.8, BC-32 and BCaC-30 which are neutral or slightly basic with a scarce surface functionalization.

The surface chemistry of supports ROX-N and ROX-NT, estimated by TPD and pH values, are in accordance with those described by other authors [17,18] using similar treatments. From Table 2, it can be also concluded that the mentioned carbons have a surface chemistry quite different from that of the original ROX-0.8 carbon.

### 3.2. Characterization of catalysts

#### 3.2.1. Adsorption isotherms

Because the anchorage of the TDA complex on the support surface can significantly modify the surface area and the pore volume, the textu-

ral properties of the heterogenized samples were also analyzed. N<sub>2</sub> adsorption isotherms at 77 K were carried out after a low temperature (323 K) outgassing treatment. Fig. 2 shows the N<sub>2</sub> adsorption isotherms for GF-45, RX-3 and BC-32 carbons and the corresponding catalysts obtained after anchoring the metal complex.

The isotherms curves shown in Fig. 2 indicate that the metal complex blocks a large amount of micropores. There is as well a clear variation in the shape of the isotherm at relative pressures lower than 0.2, which corresponds to the adsorption in the supermicropore range. In the mesopore zone ( $P/P_0$  between 0.2 and 0.7) no important changes have been found.

Table 3 shows the specific surface areas and pore volumes determined from the N<sub>2</sub> adsorption isotherm at 77 K. These data allow to quantify the carbon textural properties variations after the metal complex impregnation, indicating an important reduction of specific surface area and a considerable decrease in

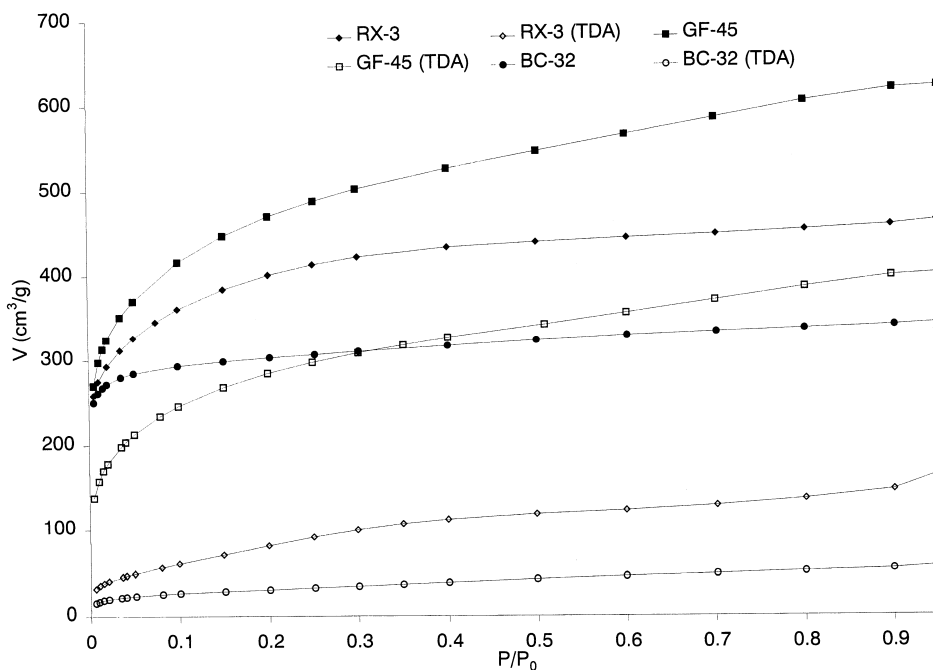


Fig. 2. N<sub>2</sub> adsorption isotherms at 77 K of carbon supports and the corresponding supported fresh catalysts.

Table 3  
Effect of the metal complex adsorption on the support porosity

Support	$S_{\text{BET}}$ (m <sup>2</sup> /g)	$\Delta S_{\text{BET}}$ (m <sup>2</sup> /g)	$V_{\text{sm}}$ (cm <sup>3</sup> /g)	$\Delta V_{\text{sm}}$ (cm <sup>3</sup> /g)	$V_{\text{meso}}^{\text{a}}$ (cm <sup>3</sup> /g)	$\Delta V_{\text{meso}}^{\text{a}}$ (cm <sup>3</sup> /g)
BC-32	935		0.088		0.042	−0.015
BC-32 (TDA)	103	−832	0.018	−0.070	0.027	
RX-3	1411		0.333		0.068	
RX-3 (TDA)	337	−1074	0.000	−0.333	0.069	0.001
GF-45	1718		0.498		0.169	
GF-45 (TDA)	961	−757	0.241	−0.257	0.171	0.002

<sup>a</sup>Only  $\varnothing = 2\text{--}7.5$  nm, obtained from N<sub>2</sub> at 77 K isotherm.

supermicropore volume. In turn, the mesopore volume variation is null or quite low (BC-32 sample).

The approximated molecular size of the metal complex was estimated in order to study its location on the support porosity. The complex bond lengths were estimated as follows: (i) Pd–N and Pd–Cl distances were taken from EXAFS studies on [Pd(NH<sub>3</sub>)<sub>2</sub>Cl<sub>2</sub>] [32] and PdCl<sub>2</sub> [33], respectively; (ii) C–N, C–C and C–H distances were taken as 1.47, 1.53, and 1.10 Å, respectively, according to those estimated for an amine and a hydrocarbon with a C–C single bond. Besides, a C–C–C bond angle of 109.5° was considered [34]. Fig. 3 shows a model of the metal complex obtained using the “Hyperchem” computer program taking into account all the numerical information and the fact that the complex has *trans*-symmetry [13]. From this model, the complex would be

approximately 4 nm long, 0.6 nm high and 0.3 nm deep. In spite of its relatively large length, the complex could reach the inner porosity when this is of slit type.

Data from N<sub>2</sub> adsorption indicate that because of the metal complex presence, the micro and supermicropores become blocked. This means that either the metal complex is totally or partially introduced in pores smaller than 2 nm, or that it is deposited on the pore entrance blocking the access.

The adsorption of the Pd–TDA complex on the support surface is suggested to take place via a Van der Waals interaction between part of the hydrocarbon chains and the carbon basal planes. According to this model, Pd and part of the hydrocarbon chain close to Pd are not in contact with the carbon surface and in this way, the electronic structure of Pd remains unchanged. Such a model, which is consistent with

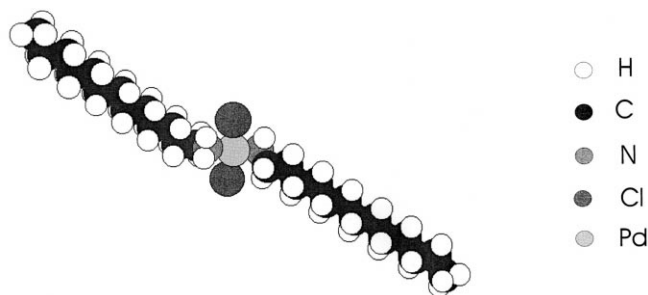


Fig. 3. Computer model of the [PdCl<sub>2</sub>(NH<sub>2</sub>(CH<sub>2</sub>)<sub>12</sub>CH<sub>3</sub>)<sub>2</sub>] complex.

Table 4

Activity results. Reaction temperature: 353 K, H<sub>2</sub> pressure: 500 kPa

Catalyst	$k_{\text{PF}} \cdot 10^{-5}$ (s <sup>-1</sup> ) <sup>a</sup>	$k_{\text{THT}} \cdot 10^{-5}$ (s <sup>-1</sup> ) <sup>a</sup>	$R_{\text{THT}}$ (%) <sup>b</sup>
Unsupported TDA <sup>c</sup>	4.20	1.45	65
TDA/ $\gamma$ -Al <sub>2</sub> O <sub>3</sub> <sup>c</sup>	5.42	1.87	65
TDA/carbon-coated $\gamma$ -Al <sub>2</sub> O <sub>3</sub> <sup>d</sup>	6.09	2.68	56
TDA/ROX-0.8	5.27	3.16	40
TDA/ROX-N	5.50	3.30	40
TDA/ROX-NT	5.41	3.01	44
TDA/BC-32	5.32	3.14	41
TDA/BCaC-30	5.30	3.29	38
TDA/RX-3	6.4	3.84	40
TDA/GF-45	7.16	4.31	40
TDA/ROX-SF	5.72	3.43	40

<sup>a</sup>Kinetic constant.<sup>b</sup> $R_{\text{THT}} = (k_{\text{PF}} - k_{\text{THT}})k_{\text{PF}}^{-1} \cdot 100$ .<sup>c</sup>From Ref. [13].<sup>d</sup>From Ref. [15].

XPS and IR data [13] was previously proposed [15].

### 3.2.2. Catalytic activity

Table 4 shows the catalytic activity ( $k$ ) and the relative decrease in activity after poisoning values ( $R_{\text{THT}}$ ) for the different catalysts in the cyclohexene hydrogenation in PF and THT conditions. For comparative purposes, Table 4 also includes the results obtained after evaluation of the unsupported TDA complex and the TDA complex supported on  $\gamma$ -Al<sub>2</sub>O<sub>3</sub> [13] and on carbon-coated  $\gamma$ -Al<sub>2</sub>O<sub>3</sub> [15]. From these data, it shows that all the supported catalysts are more active than the unsupported metal complex. However, there are noticeable variations in the catalytic activity depending on the carbon support used. The catalytic activity in the PF condition increases by 38% when comparing the less and the most active supported catalyst. On the other hand, all the catalysts suffer a loss of activity in THT conditions. The results of Table 4 also show that the catalysts supported on

Table 5

XPS results. Reaction temperature: 353 K, H<sub>2</sub> pressure: 500 kPa

Catalyst	Reactant solution	Pd 3d <sub>5/2</sub> (eV)	N 1s <sub>1/2</sub> (eV)	Cl 2p (eV)	N/Pd (at./at.)	Cl/Pd (at./at.)	S 2p (eV)	S/Pd (at./at.)
Unsupported TDA	Fresh	338.2	402.0	198.2	2.00	2.00	–	–
TDA/ROX-0.8	PF	338.1	401.9	198.1	1.99	2.01	–	–
	THT	338.3	402.1	198.0	1.00	2.01	163.0	0.64
	Fresh	338.3	402.1	198.2	2.00	1.98	–	–
TDA/ROX-N	PF	338.2	402.0	198.1	2.01	1.99	–	–
	THT	338.5	402.0	198.2	1.01	2.00	162.9	0.65
	Fresh	338.3	402.0	198.0	2.01	2.02	–	–
TDA/ROX-NT	PF	338.4	401.9	198.1	1.98	2.00	–	–
	THT	338.4	401.8	198.1	1.01	2.01	163.1	0.63
	Fresh	338.2	401.8	198.2	2.02	2.02	–	–
TDA/ROX-SF	PF	338.2	402.2	198.1	2.00	2.01	–	–
	THT	338.5	401.9	198.0	1.00	2.00	163.0	0.63
	Fresh	338.4	401.9	198.2	2.00	2.00	–	–
TDA/RX-3	PF	338.3	402.0	198.0	2.01	1.99	–	–
	THT	338.4	401.9	198.1	0.97	2.00	162.8	0.63
	Fresh	338.2	402.0	198.2	2.01	1.98	–	–
TDA/BC-32	PF	338.3	401.8	198.1	2.00	2.00	–	–
	THT	338.4	402.0	198.3	1.01	2.02	163.0	0.65
	Fresh	338.2	401.9	198.0	1.97	2.00	–	–
TDA/GF-45	PF	338.2	401.9	197.9	1.99	2.01	–	–
	THT	338.4	402.0	198.1	0.96	2.00	162.9	0.64
	Fresh	338.4	401.9	198.2	2.00	1.98	–	–
TDA/BCaC-30	PF	338.4	402.0	198.1	2.01	1.98	–	–
	THT	338.3	402.0	197.9	0.94	2.00	163.1	0.64



carbons are more sulphur-resistant than those supported on alumina, coated- $\text{Al}_2\text{O}_3$  and also than the unsupported metal complex. The relative loss of activity for the carbon-supported catalysts is around 40% in all cases, meaning perhaps, that it does not depend on the carbon properties. The capability of carbon to adsorb the poison was tested and it was found that THT does not adsorb on the selected carbon supports.

### 3.2.3. X-ray photoelectron spectroscopy

Table 5 presents the Pd  $3d_{5/2}$ , N  $1s_{1/2}$ , Cl 2p and S 2p peaks binding energies (BE) and the atomic ratios N/Pd, Cl/Pd and S/Pd obtained for the supported and unsupported  $[\text{PdCl}_2(\text{NH}_2(\text{CH}_2)_{12}\text{CH}_3)_2]$  complex, fresh and after having been used in the catalytic activity tests (with and without poison). For every supported catalyst, the Pd/C surface atomic ratio was almost the same: 0.073, and the C 1s peak BE was 285.0 eV, which corresponds to graphite.

The results show that the Pd  $3d_{5/2}$ , Cl 2p and N  $1s_{1/2}$  peaks BE and the atomic ratios N/Pd and Cl/Pd measured for the fresh supported metal complex samples and the unsupported one are almost the same. As previously reported [13], the ratios found are those corresponding to the theoretical stoichiometry in the  $[\text{PdCl}_2(\text{NH}_2(\text{CH}_2)_{12}\text{CH}_3)_2]$  molecule. In agreement with the electronic state that could be expected for the metal complex under study, the position of the N  $1s_{1/2}$  and Cl 2p peaks corresponds, in all cases, to nitrogen in an amine and to chloride species, respectively [13]. The presence of surface Pd electrodeficient species can be suggested; this is in agreement with the position of the Cl 2p peak. According to these results, the palladium complex is tetra-coordinated and even supported, it maintains this coordination. This indicates that the Pd complex keeps its chemical identity after heterogeneization.

Data of Table 5 indicate a clear effect of the poison presence in the state of the Pd. The most clear changes are a decrease in the coordination by N and that there is some coordination by S.

These results are in concordance with the previous work [14,15].

## 4. Discussion

The catalytic activity results for catalysts obtained from ROX-0.8, ROX-N and ROX-NT were used to study the possible effect of the support surface chemistry. The selection was based on the different amount of oxygen groups present in these samples (Table 2). These carbons share, however, a similar specific surface area (around  $940 \text{ m}^2/\text{g}$ ) and pore size distribution (Table 1). That is, treatments used to obtain the derived carbons from ROX-0.8 affect slightly the carbon pore structure [17].

Fig. 4 presents catalytic activity ( $k_{\text{PF}}$ ) vs. the total amount of micromoles of CO and  $\text{CO}_2$  determined by a TPD experiment. The small increase in catalytic activity measured for the samples with considerable increasing of CO and  $\text{CO}_2$  micromole numbers is so slight that can be considered within the experimental error. Because of that, it can be thought that the oxygen surface groups do not act as anchoring centres for the metal complex nor for reactants ( $\text{H}_2$  and/or cyclohexene). It has been widely reported [2,4,35–42] that in order to improve the anchoring of the metal complex on the support surface, this one should be submitted to previous functionalization treatments to create N, P, S or O containing groups. In our case, it seems that the anchoring takes place by Van der Waals interactions between the ligand aliphatic chains (TDA) and graphitic planes, edges or corners and the oxygen groups do not influence it. Besides, no washing of the metal complex in the reaction conditions was observed [13]. That is, the metal complex is effectively fixed without the necessity of a support specific pre-treatment. On the other hand, the XPS results indicate that there are no interactions between Pd and any atom from the support (oxygen or

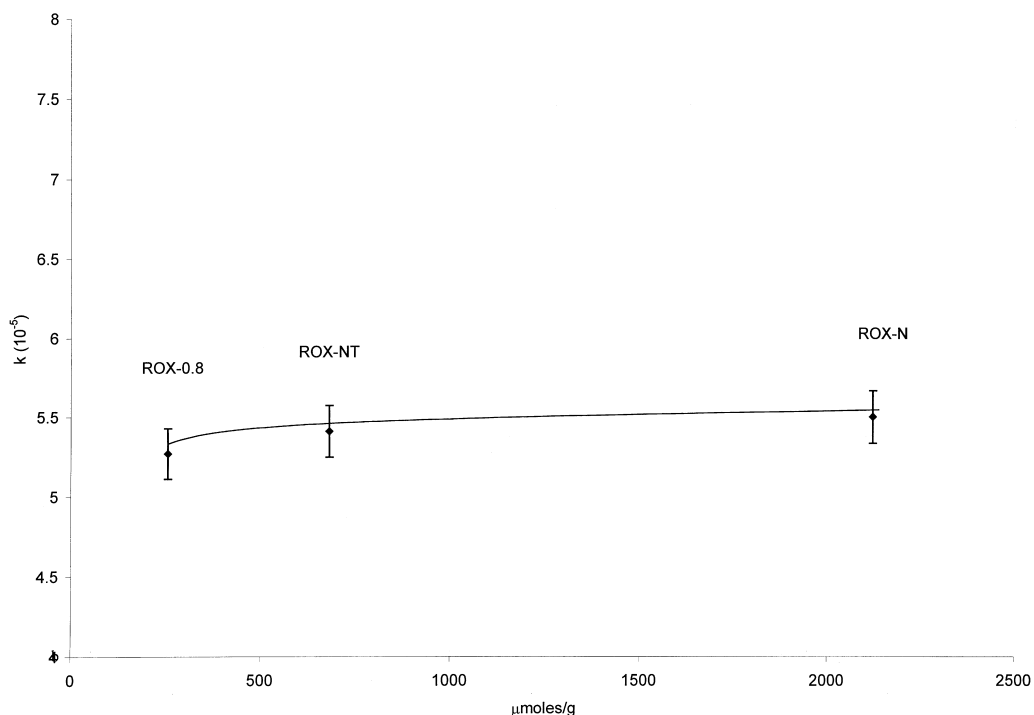


Fig. 4. Catalytic activity in PF conditions (expressed as rate constant  $k_{PF}$ ) vs. the support surface chemistry (as  $\mu\text{mol}$  of CO and CO<sub>2</sub> evolved in a TPD experiment).

carbon), confirming the previous hypothesis. Besides, the absence of surface oxygen groups effect in the catalytic activity suggests that they do not act as adsorption centres for the reactants, H<sub>2</sub> and/or cyclohexene.

The  $k_{PF}$  values in Table 4 were related to the different carbon porosity ranges, trying to find any connection between these two variables. Results obtained for the catalysts prepared with ROX-N and ROX-NT were not included because their porosity is quite similar to that of the parent ROX-0.8. Due to comments made in Section 3.2.1, it is important to remark that the narrower micropores must have no effect on the catalytic activity. Figs. 5–7 show the variation of  $k_{PF}$  vs. supermicro-, meso-, and macropore volumes, respectively. It can be observed that only the plot of  $k_{PF}$  vs. supermicropore volume (Fig. 5) shows a clear linear relationship between both parameters (catalytic activity and

pore volume). Besides, it can be observed that for  $V_{sm}$  lower than 0.1 cm<sup>3</sup>/g, there is no dependence of  $k_{PF}$  with the pore volume. This is the case of the catalysts prepared with carbon BC-32 and of some other samples reported previously [14] prepared with chars of phenol-formaldehyde resin. The mentioned carbons have quite a low volume of supermicropores and the metal complex is likely located in the smaller mesopores.

The metal complex is expected to be anchored in the smaller accessible pores. This can be explained, considering that the narrower the pore is, the larger the adsorption potential will be [43,44]. Although the metal complex is a long molecule, the aliphatic chains can be deformed quite easily by bond rotation; hence, its real dimensions are not easy to know. In any case, it can be shorter in the adsorbed state. The location of the metal complex in the supermi-

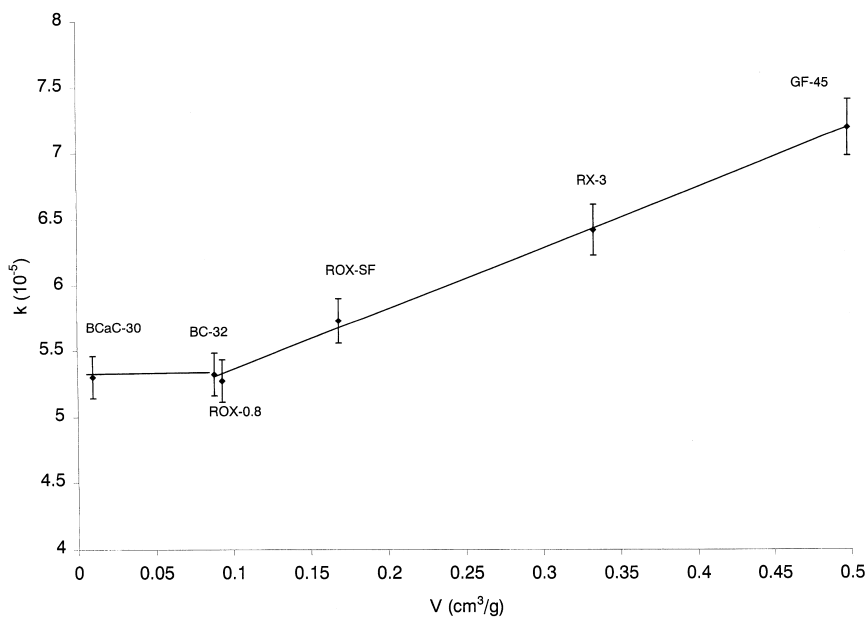


Fig. 5. Catalytic activity in PF conditions (expressed as rate constant  $k_{PF}$ ) vs. the supermicropore volume of the carbon supports.

ropores, originates zones with a high reactants concentration around the anchored metal com-

plex. In this way, a larger supermicropore volume will provide better complex dispersion,

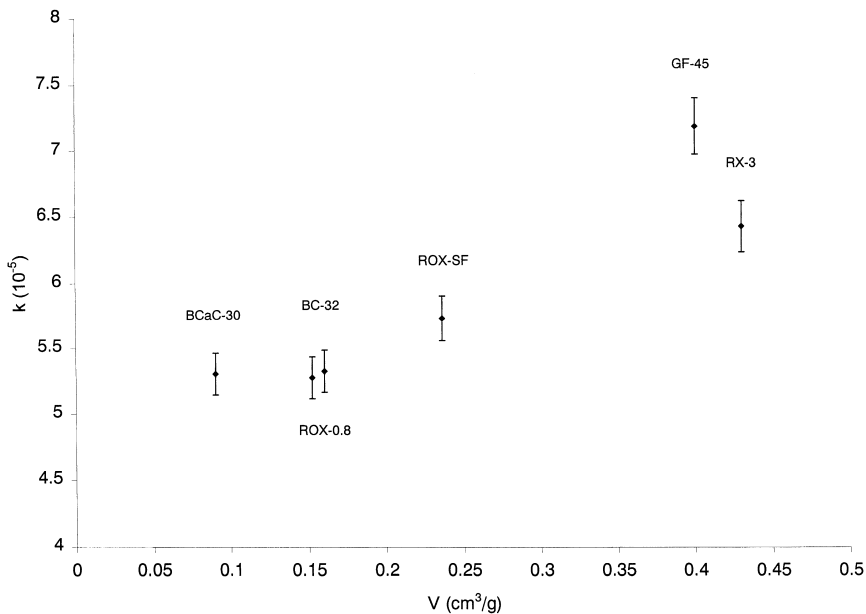


Fig. 6. Catalytic activity in PF conditions (expressed as rate constant  $k_{PF}$ ) vs. the mesopore volume of the carbon supports.

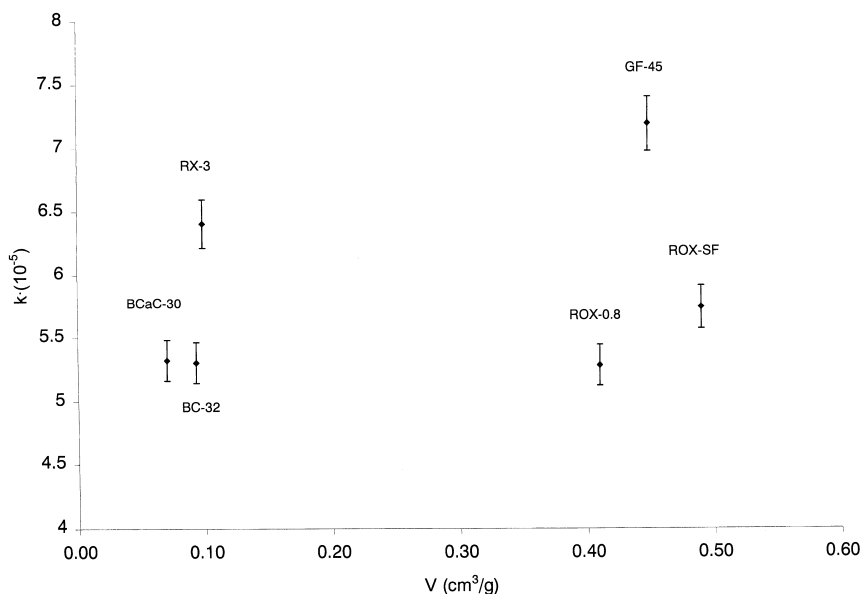


Fig. 7. Catalytic activity in PF conditions (expressed as rate constant  $k_{\text{PF}}$ ) vs. the macropore volume of the carbon supports.

what will, in turn, allow a larger number of sites where the reactants can concentrate with the consequent ease of reaction.

If the reaction were controlled by pore diffusion mechanism, there would be a macro- or mesopore volume dependence, as it was observed in hydroformylation reaction using Rh-complexes [44]. In our case, although there is some positive tendency between activity and  $V_{\text{meso}}$ , it is quite at random.

Organic sulphur and ashes present in carbons may have an important effect on the catalyst properties when they are used as supports [19,45]. Data from Table 2 show that ROX-0.8, ROX-N, ROX-NT and RX-3 carbons have some S content. ROX-0.8 was treated to remove sulphur (Section 2.1) and so to determine the effect of that component. Activity results shown in Fig. 5, referred to catalysts prepared with ROX-0.8 and ROX-SF supports, indicate that there is no effect due to the presence of sulphur in the support. The catalytic activity rise, after sulphur removal, was based on the supermicropore volume increase, following the same tendency than

the rest of the supports. Although the ROX-0.8 carbon has some sulphur content, this value is not excessive, and so other authors [17,44] used it as catalyst support. In this specific case, it can be said that the carbon sulphur content does not affect the catalytic activity.

From Table 4, it can be observed that the  $R_{\text{THT}}$  values are around 40% for catalysts supported on carbon and that they are independent of the active carbon used (source, surface area, surface chemistry, elemental composition, etc.). Comparing these results with those obtained for the: (a) unsupported metal complex, (b) metal complex supported on  $\gamma\text{-Al}_2\text{O}_3$ , and (c) metal complex supported on a carbon coated  $\gamma\text{-Al}_2\text{O}_3$  [13–15], it can be observed that in the first two cases, the catalytic activity diminution was around 65%, larger than the 40% obtained for the carbons. This also suggests, that in case (b) the support ( $\gamma\text{-Al}_2\text{O}_3$ ) does not alter the poison behaviour in relation to the metal complex, while the carbon supports have some influence on the poisoning mechanism. Another result that supports these conclusions is the fact that

there is an intermediate resistance to THT in case (c) (carbon coated  $\gamma$ -Al<sub>2</sub>O<sub>3</sub>) [15].

The results presented in Table 5 show that there were no changes in the catalysts properties analyzed by XPS after impregnation or catalytic test in the PF solution (Table 5). However, after reaction in the THT solution, a sulphur peak was detected at 162.9 eV, which may be attributed to sulphur in THT [14], which is the actual poisoning species. A decrease in the atomic ratio N/Pd (of approximately 50%) in the presence of poison was observed for all the supported catalysts, while the Cl/Pd ratio remained practically constant (Table 5). This suggests that the poisoning mechanism of the palladium complex by THT is by the insertion of the poisoning molecule into the coordination sphere of palladium to form a Pd–S bond. This behaviour was previously observed with other supports [13–15]. Data of Table 5 indicate that THT molecules might substitute approximately half of the amine ligands, generating less active species. That is, in carbon-supported poisoned catalysts, the ratio S/Pd is around 0.6, while the ratio N/Pd is 1 (instead of 2, that corresponds to the stoichiometry of the original complex). This result has been found only when carbonaceous materials are used as supports. With  $\gamma$ -Al<sub>2</sub>O<sub>3</sub> the ratio S/Pd in poisoned catalysts was also 1. These XPS results need a deeper study. In previous works [13], we have reported that when thiophene is used as poison, such a substitution does not occur, which is probably the reason why THT has a greater poisoning effect than thiophene.

Having in mind and assuming that: (i) the THT poisoning mechanism implies a substitution of the complex amine ligand [14,15]; (ii) the aliphatic amine chains have a strong interaction with the surface support [4] and (iii) the aliphatic chain–carbon surface interaction is stronger (by chemical affinity, as reported in the case of aromatic ligands [46]) than the aliphatic chain–alumina surface, it is proposed that the higher resistance to poison found with carbon supports may be attributed to a higher metal

complex stabilization and, hence, an extra difficulty for the substitution of the THT molecule.

## 5. Conclusions

Results obtained using a series of active carbons with different textural properties and surface chemistry allow us to conclude the following:

- The anchoring of the [PdCl<sub>2</sub>(NH<sub>2</sub>-(CH<sub>2</sub>)<sub>12</sub>CH<sub>3</sub>)<sub>2</sub>] complex on the active carbon surface takes place by the physical adsorption of the long ligand aliphatic chain on the carbon basal planes, edges or corners, and not due to interaction with the surface oxygen groups. The interaction (of the Van der Waals type) is strong due to the long ligand aliphatic chain.
- Because of the strong metal complex–carbon adsorption, the [PdCl<sub>2</sub>(NH<sub>2</sub>(CH<sub>2</sub>)<sub>12</sub>CH<sub>3</sub>)<sub>2</sub>] complex remains stabilised and presents a higher THT poisoning resistance than the metal complex unsupported or supported on  $\gamma$ -Al<sub>2</sub>O<sub>3</sub>.
- The metal complex is adsorbed on the carbon material in the supermicropores porosity range.
- The catalytic activity is found to linearly depend on the supermicropore volume. A larger supermicropore volume implies a better complex dispersion and an increase of sites where the reactant concentration around the metal complex is higher than in bulk solution.

## Acknowledgements

We are indebted to UNL (CAI + D Program) and CICYT (AMB96-0799) for partial financial support and to JICA for the donation of the XPS equipment. We thank S. de Miguel and his group for the preparation of ROX-SF support.

## References

- [1] J. Barbier, E. Lamy-Pitara, P. Marecot, J.P. Boitiaux, J.P. Cosyns, F. Verna, *Adv. Catal.* 37 (1990) 279.
- [2] L.M. Tang, M.V. Huang, Y.Y. Jiang, *Macromolecules* 15 (1994) 527.
- [3] L.V. Nosova, V.I. Zikovskii, Yu.A. Ryndin, *React. Kinet. Catal. Lett.* 53 (1994) 131.
- [4] V.M. Frolov, *Platinum Met. Rev.* 40 (1996) 8.
- [5] H. Bricout, J.F. Carpentier, A. Montreux, *J. Chem. Soc.* 18 (1985) 1863.
- [6] T.P. Voskresenskaya, V.D. Chinakov, V.N. Nkekipelov, A.V. Mshkina, *React. Kinet. Catal. Lett.* 32 (1986) 359.
- [7] P. Barbaro, P.S. Pregosin, R. Saltzman, A. Albninati, R.W. Kunz, *Organometallics* 14 (1995) 5160.
- [8] S.B. Eremburg, N.V. Bansk, L.N. Mazalov, M.K. Drozdora, V.T. Torgot, *J. Struct. Chem.* 36 (1995) 941.
- [9] E.M. Kar'Kova, A.V. Novikova, L.E. Rozantseva, V.M. Frolov, *Kinet. Catal. Lett.* 32 (1993) 866.
- [10] V.M. Frolov, D.P. Parenago, A.V. Novikova, L.S. Kovaleva, *React. Kinet. Catal. Lett.* 25 (1984) 319.
- [11] G.M. Cherkasin, L.P. Shuikina, D.P. Parenago, V.M. Frolov, *Kinet. Catal.* 26 (1985) 1110.
- [12] A. Rakai, D. Tessier, F. Bonzon-Verduraz, *New J. Chem.* 16 (1992) 869.
- [13] P.C. L'Argentièrre, D.A. Liprandi, E.A. Cagnola, N.S. Fígoli, *Catal. Lett.* 44 (1997) 101.
- [14] P.C. L'Argentièrre, D.A. Liprandi, E.A. Cagnola, M.C. Román-Martínez, C. Salinas-Martínez de Lecea, *Appl. Catal. A: Gen.* 172 (1998) 41.
- [15] C. Salinas-Martínez de Lecea, A. Linares-Solano, P.C. L'Argentièrre, *Carbon* 38 (2000) 157.
- [16] M. Almela-Alarcón, PhD Thesis, Universidad de Alicante, Spain, 1988.
- [17] H.E. Van Dam, H. Van Bekkum, *J. Catal.* 131 (1991) 335.
- [18] M.C. Román-Martínez, D. Cazorla-Amorós, A. Linares-Solano, C. Salinas-Martínez de Lecea, *Carbon* 31 (1993) 895.
- [19] G. Torres, E. Jablonski, A. Castro, S. De Miguel, O. Scelza, M. Blanco, M. Peña, J. García-Fierro, *Appl. Catal., A* 161 (1997) 213.
- [20] F. Rodríguez-Reinoso, A. Linares-Solano, in: P.L. Walker Jr. (Ed.), *Chemistry and Physics of Carbon 21* Marcel Dekker, New York, 1988, p. 1.
- [21] M.M. Dubinin, L.V. Radushkevich, *Zhur. Fiz. Khim.* 23 (1949) 69.
- [22] S. Brunauer, P.H. Emmet, E. Teller, *J. Am. Chem. Soc.* 60 (1938) 809.
- [23] A. Linares-Solano, C. Salinas-Martínez De Lecea, D. Cazorla-Amorós, J.P. Joly, M. Charcoset, *Energy and Fuels* 4 (1990) 467.
- [24] H.P. Boehm, *High Temperature High Pressure* 22 (1990) 275.
- [25] M.C. Román-Martínez, D. Cazorla Amorós, A. Linares-Solano, C. Salinas-Martínez de Lecea, H. Yamashita, M. Anpo, *Carbon* 33 (1994) 3.
- [26] X.L. Seoane, P.C. L'Argentièrre, N.S. Fígoli, A. Arcoya, *Catal. Lett.* 16 (1992) 137.
- [27] F.A. Holland, F.S. Chapman, *Liquid Mixing, Processing in Stirred Tanks*, Reinhold, New York, 1976, Chap. 5.
- [28] C. Niklasson, C. Anderson, N.H. Schoon, *Ind. Chem. Res.* 26 (1987) 1495.
- [29] T. Mallat, J. Petro, T. Szabó, J. Sztatisz, *React. Kinet. Catal. Lett.* 29 (1985) 353.
- [30] R. Prada Silvy, J.M. Beuken, J.L.G. Fierro, P. Bertrand, B. Delmon, *Surf. Interface Anal.* 8 (1986) 167.
- [31] R. Borade, A. Sayari, A. Adnot, S. Kaliaguine, *J. Phys. Chem.* 94 (1990) 5989.
- [32] B.L. Mojet, M.S. Hoogenraad, A.J. Dillen, J.W. Geus, D.C. Koningsberger, *J. Chem. Soc., Faraday Trans.* 93 (24) (1997) 4371.
- [33] D. Bazin, A. Triconnet, P. Moureaux, *NIM B* 97 (1995) 41.
- [34] K. Peter, C. Volhardt, *Organic Chemistry*, VCH Publishers, New York, 1986.
- [35] C.U. Pittman, B.T. Kim, W.M. Douglas, *J. Org. Chem.* 40 (5) (1975) 590.
- [36] J.A.C. Alves, C. Freire, B. De Castro, J.L. Figueiredo, in: *Extended Abstracts International Carbon Conference*, Strasbourg, France, 1998, p. 153.
- [37] Y.I. Ermakov, V.A. Likholobov, *Kinet. I Katal.* 21 (5) (1980) 1208.
- [38] A.M. Trzeciak, J.J. Ziolkowski, Z. Jawrska-Galas, W. Mista, J. Wryszcz, *J. Mol. Catal.* 88 (1994) 13.
- [39] T. Okano, T. Kobayashi, H. Konishi, J. Kiji, *Bull. Chem. Soc. Jpn.* 55 (1982) 2675.
- [40] R.J.C. Osbaldiston, E.J. Markel, *J. Mol. Catal.* 91 (1994) 91.
- [41] J.P. Mathew, M. Srinivasan, *Polymer International* 31 (1993) 119.
- [42] S.D. Nayak, V. Mahadevan, M. Srinivasan, *J. Catal.* 92 (1985) 327.
- [43] J.H. de Boer, J.F.H. Custers, *Z. Phys. Chem. (B)* 25 (1934) 225.
- [44] T.A. Kainulainen, M.K. Niemelä, A.O.I. Krause, *J. Mol. Catal. A: Chem.* 122 (1997) 39.
- [45] S.R. de Miguel, G. Torres, A.A. Castro, O. Scelza, *React. Kinet. Catal. Lett.*, 51 (1993) 2, 443.
- [46] A.A. Keterling, A.S. Lisitsyn, V.A. Likholobov, A.A. Gall', A.S. Trachum, *Kinet. Catal.* 31 (1990) 1273.